Virtual Design of LIGA Fabricated Meso Scale Gas Bearings for Microturbomachinery

Daejong Kim
Texas A&M University, Department of Mechanical Engineering
3123 TAMU, College Station, TX 77843, U.S.A.

Abstract

This paper introduces a virtual design and manufacturing process of mesoscale flexure pivot tilting pad and foil gas bearings made of metal with diameter of 5mm and high L/D ratio (>0.5). Proposed manufacturing process is a LIGA process involving X-ray lithography and electroplating. Virtual design studies involve time domain stability analyses for accurate prediction of dynamic performance. Simulation studies indicate much higher potential of tilting pad gas bearing over foil bearings, which are less stable than tilting pad bearing. Design features of the gas bearings that can be fabricated via LIGA process and their advantages over precision-machined ones are discussed in terms of design flexibility and repeatability.

Keywords: PowerMEMS, Gas bearing, LIGA, Stability

1 - INTRODUCTION

Mesoscale microturbomachinery for power generation require usage of gas bearings to minimize frictions at high speeds. An approach using silicon as a structural material for the gas bearings constrains design features to solid wall geometry [1] with limited performance. Furthermore, structural and manufacturing limitations of the silicon microturbomachinery mandate very small L/D (length to diameter) ratio of the micro gas bearings. Operation of the silicon micro gas bearings often requires hydrostatic pressurization for stability, which complicates overall flow path and may not feasible in certain microturbomachinery applications. A miniaturization of existing small turbomachinery to mesoscale microturbomachinery, of which example can be found in [2], can eliminate the structural limitation inherent to the silicon microturbomachinery. This approach can reduce the rotor speed below 1,000,000 rpm because the impeller size can be increased up to 10~12mm for bearing size of 5~6mm. For these scales, gas bearings made of metals with high rotor-bearing stability are preferred.

2 - PRINCIPLE OF FOIL AND TILTING PAD GAS BEARINGS

Figure 1 shows a schematic of foil gas bearing. Continuous corrugated bump foil supports the smooth top foil which generates hydrodynamic pressure upon rotor spins. The microscopic slips of bump foils with the top foil and bearing sleeve generate Coulomb frictional damping necessary for stable operation. Furthermore, the compliant structure of the foil bearing can accommodate rotor-bearing misalignment and debris very effectively. Precision-made mesoscale foil bearings and their operating characteristics are reported in [3,4]. Figure2 shows principle of tilting pad gas bearing and photo of EDM (Electro discharge machining) machined macro scale (bearing diameter of 28mm) flexure pivot tilting pad bearings. Hydrodynamic preload r_p is defined as a ratio of the distance between O_J and O_P in Fig. 2 and nominal clearance C. Therefore the bearing set bore clearance becomes C(1-r_p). Time domain and frequency domain stability analyses on the flexure pivot tilting pad gas bearing in Fig.2 can be found in [5,6].

The radial compliance (shown as a straight beam behind the flexure pivot) was implemented to accommodate rotor centrifugal and thermal growth. The geometries of flexure pivot tilting pad gas bearing and foil bearing are 2-D in nature and a MEMS process that can produce high aspect microstructures can be used to make these types of gas bearings. However, due to continuous elastic motion of bump foils and flexure pivots during the operation, semi-conductor materials are excluded in the consideration of material selection. Furthermore, geometrical accuracy and very smooth bearing surface are crucial for proper functions. LIGA (German Acronym for Lithography, Electroplating and Molding) process involving X-ray lithography is a natural selection of the process to manufacture these advanced micro gas bearings using metals. Micro scale gas bearings fabricated using LIGA process has been reported earlier [7] and the process can be applied to mesoscale gas bearings.

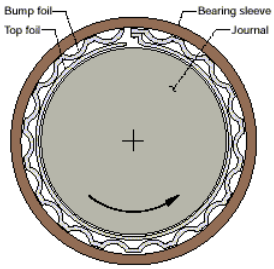

Figure 1 - Schematics of foil gas bearing [8]

3 - MANUFACTURING PROCESS

LIGA process involves X-ray lithography on X-ray sensitive photo resist such as PMMA or SU-8, electroplating of a metallic mold insert, and replication of plastic micro part using the metallic mold insert. The molded plastic part can be used as plating mold of metallic microstructure, enabling replication of metallic microstructure without repeating expensive X-ray lithography. X-ray lithography uses X-ray with extremely small wavelength (0.2~0.4nm), providing capability of micro manufacturing of very high aspect ratio structure. For microstructure with 1mm height, a typical deviation from vertical sidewall is about 1μm [9].

Figure 3 shows a design of mesoscale (D=5mm, L=4mm) flexure pivot tilting pad gas bearing with foil damper. In the

figure, tilting pads and arc beam springs and foil dampers are made as a monolithic structure and assembled into precision machined bearing sleeve. To achieve high L/D ratio, 4 layers of 1mm thick metallic structures are stacked together and eutectic-bonded using aligning pins and bonding layers such as thin Au films. The locations of aligning pins are in the pads and high pressure is applied to bond the bearing layers. Because pad springs and foil dampers are not required to be bonded, pressure is applied only on the pads. Alternative fabrication process could be a manufacturing very thick bearing layer (up to 2.5mm, rendering L/D=0.5) using single X-ray lithography process to avoid aligning and bonding issue.

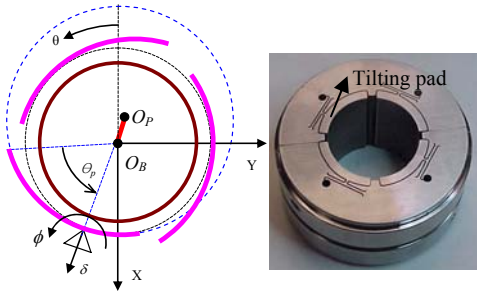

Figure 2 – Principle of tilting pad gas bearing and EDM machined 4 pads flexure pivot tilting pad gas bearing

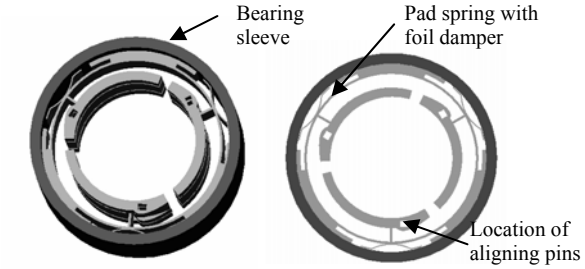

(a) 3D view (b) Top view

Figure 3 – Mesoscale flexure pivot tilting pad gas bearing with foil damper

Fabrication of foil bearing starts with multiple layers of bump foils, which are inserted into precision wire EDM machined bearing sleeve. Bump foil layers are not required to be bonded each other because they are elastic foundation to a precision-formed top foil (Fig. 4). The slot necessary for assembly of top foil can be made during the LIGA process of the bump foils. Unique feature of tilting pad and foil gas bearings that can be achieved through LIGA process is a capability to fabricate various compliant wall structures that cannot be made via traditional precision machining processes. For example, radial pad spring with foil damper is a unique feature of proposed mesoscale tilting pad bearing. The foil damper provides Coulomb damping to the tilting pad improving rotor-bearing stability. Each bump in Fig. 4 provides independent stiffness and damping to top foil unlike macro scale foil bearings shown in Fig.1. The LIGA process can fabricate bumps with different stiffness and damping characteristics along the circumferential and axial directions by engineering each bump independently.

LIGA process involves electroplating of metal (mostly Ni) in Sulfamate bath or Watts bath due to low residual stress. As reported in [10,11], annealing of the Sulfamate and Watt Ni above 500°C embrittles the materials and cannot be used as a structural load-bearing components. To avoid the embrittlement and maintain excellent mechanical properties of as-plated Ni, electro co-deposition of various alloying materials such as Mn [11] or ceramic particles [12] have been reported. These alloying materials hinder grain growth which is one of the main causes of degradation of mechanical properties. The proposed gas bearings are to be made via electroplating of Ni-Mn alloy or Ni-ceramic nanocomposites.

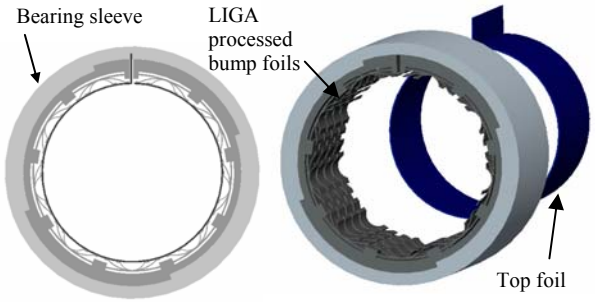

(a) Top view of assembled foil bearing (b) Assembly scheme

Figure 4 – Proposed fabrication process of mesoscale foil bearing using LIGA process

4 - DESIGN STUDIES

High speed operation of micro turbomachinery induces rotor centrifugal growth which should be considered when gas bearing is designed. The centrifugal growth can be estimated from plane stress model [13], given by

$$r_g = \left[(1-\nu)RC_0 - (1+\nu)C_1/R - \rho_r\Omega^2R^3(1-\nu^2)/8\right]/E \quad (1)$$

$$C_0 = \rho_r\Omega^2(a^2+R^2)(3+\nu)/8, \quad C_1 = -\rho_r\Omega^2a^2R^2(3+\nu)/8$$

, where ρ_r, E, ν are density, Young's modulus, and Poison's ratio of the rotor material, respectively, and a is an inner radius of the rotor. Eq. (1) agrees very well with finite element analyses results [5]. The parabolic function of Eq. (1) with Ω indicates a significant rotor centrifugal growth at high speeds, often exceeding the bearing clearance. The intended purpose of the radial compliance in tilting pad gas bearing was to accommodate the large rotor centrifugal growth.

In the linear stability analyses, excitation frequency-dependent bearing impedance is calculated at specific operating speed. As excitation frequency changes, when modal damping changes its sign from positive to minus, the operating speed is can be considered unstable assuming external disturbance has a frequency component that renders the modal damping zero. However, as shown in [14], the linear stability analyses provide only bearing natural frequency at given operating speed and does not provide exact onset speed of instability. The author shows that only orbit method can predict both natural frequency and onset speed of instability accurately [14]. In this paper, stability characteristics and overall bearing performance are evaluated using orbit method to provide better insight on rotor-bearing instability. Time domain orbit methods solve multiple differential equations associated with pressure field, rotor motion, and dynamics of bearing surface (tilting pads and

bump foils) simultaneously. Unsteady Reynolds Equation, given by Eq. (2),

$$\frac{\partial}{R\partial\theta}\left(\frac{ph^3}{12\mu}\frac{\partial p}{R\partial\theta}\right)+\frac{\partial}{\partial z}\left(\frac{ph^3}{12\mu}\frac{\partial p}{\partial z}\right)=\frac{U}{2}\frac{\partial}{R\partial\theta}(ph)+\frac{\partial}{\partial t_s}(ph), \quad (2)$$

Equations of rotor radial motions are given by

$$m_r\ddot{e}_X = F_X + m_r u_{im}\omega^2\cos\omega t + m_r g, \quad (3a)$$

$$m_r\ddot{e}_Y = F_Y + m_r u_{im}\omega^2\sin\omega t, \quad (3b)$$

where m_r is a rotor mass, u_{im} is an imbalance radius, g is a gravity constant, and F_X and F_Y are dynamic bearing reaction forces to the rotor. Dynamic equation of bump deflection is described as

$$f_b = k_b u + c_b\dot{u}. \quad (4)$$

Here, the f_b is a pressure force on a bump given by $f_b = pA_0$, where A_0 is an effective area that the bump covers. The k_b is the bump stiffness and c_b is equivalent bump viscous damping coefficient of Coulomb damping at friction interfaces. Many empirical studies on macro scale foil bearings [15-17] shows the curved bump structure can be modeled as a viscous damping with structural loss factor of around 0.15. In the simulations, the loss factor of 0.15 is used for every bump. For tilting pad gas bearings, pad tilting motion and pad radial motion can be described as

$$I_P\ddot{\phi}_i + k_\phi\phi_i = M_{i\phi}, \quad (5a)$$

$$m_P\ddot{\delta}_i + c_\delta\dot{\delta}_i + k_\delta\delta_i = F_{i\delta}, \quad (5b)$$

where index i represents pad number, $M_{i\phi}$ and $F_{i\delta}$ are tilting moment and radial force to the i^{th} pad. Coulomb damping of foil damper in the tilting pad bearing is also approximated as equivalent viscous damping coefficient with structural loss factor of 0.15. Gas film thickness is a function of rotor motion and deflection of bearing surface. For tilting pad bearings, film thickness considers rotor centrifugal growth, r_g, tilting angle, ϕ, pad radial displacement, δ, and hydrodynamic preload, r_p

$$h(\theta) = C - r_g + e_X\cos\theta + e_Y\sin\theta - \phi R\sin(\theta-\theta_p) - (r_p C-\delta)\cos(\theta-\theta_p), \quad (6)$$

where R is a bearing radius and θ_p is a location of pivot. For foil bearing, film thickness function is described as

$$h((\theta,Z) = C - r_g + e_X\cos\theta + e_Y\sin\theta + u(\theta,z). \quad (7)$$

In both Eqns. (6) and (7), e_X and e_Y are eccentricities of journal center along the X and Y directions. The 5th order Adams-Bashforth scheme [18] solves Eqs. (2)~(5) in time domain. Detailed procedure for orbit simulation of foil gas bearing can be found in [14]. Rotor mass for the simulations is 10g.

5 - RESULTS AND CONCLUSION

Design variables are tilting stiffness, radial stiffness, stiffness portion of foil damper, pad offset, preload, nominal bearing clearance, number of pads, pad mass, and pad moment of inertia. Because of so many design variables, design optimization requires arbitrary selection of several design variables which are relatively insensitive to the rotor-bearing instability. Previous design studies on macro scale flexure pivot tilting pad gas bearing [5,6] provides guidelines for selecting initial variables. Table 1 shows selected design parameters considering minimum feature size of 80μm (i.e., thickness of foil damper) that can be fabricated through the LIGA process. The bearing length of 4mm indicates four 1mm thick bearing layers two 2mm thick bearing layers are required to be bonded.

Figure 5 shows selected non-dimensional imbalance responses at steady states up to 800,000 rpm assuming operating speed is below first bending critical speed. Critical speed (low frequency oscillations) predicted from time trace of ε_X in Fig. 6 is below 100,000 rpm.

Table 1 Selected design variables for tilting pad gas bearing

Parameters	SI unit	
Number of pads	3	
Pad arc length	110	degree
Pivot offset	0.7	
Preload (r_p)	0.5	
Tilting stiffness (k_ϕ)	4.35×10^{-2}	Nm/rad
Total radial stiffness	5.74×10^{6}	N/m
Bearing radius (R)	2.5	mm
Bearing length (L)	4	mm
Rotor mass (m_r)	0.01	kg

Design parameters of foil gas bearings are bump stiffness variations along the circumferential and axial directions, and bearing nominal clearance. Parametric design studies on macro scale foil bearing [14] show that rotor-bearing stability and load capacity is relatively insensitive to bump stiffness variation. In the proposed mesoscale foil bearing, all the bumps have identical stiffness. A series of simulations for design optimization were required to achieve maximum threshold speed. Interestingly enough, foil bearing has less stability than tilting pad bearings when the bearing is loaded by rotor weight only. Not shown in this article is much larger cross-coupled stiffness of foil gas bearing than flexure pivot tilting pad bearing. Existence of damping in the underlying elastic foundation is offset by large load capacity, which leads to almost centered rotor position and generation of large cross-coupled stiffness. However, loading of the bearing increases stability significantly. Figure 7 shows time trace of loaded (0.5N) foil bearing at 500,000 rpm. The low frequency component corresponds to natural frequency of the bearing superimposed by synchronous imbalance components. Loaded bearing was stable up to 620,000 rpm. Optimized foil bearing clearance is about 3 times lager than tilting pad bearing allowing easy assembly. However, considering the requirement of (presumably) very tight tip clearance of impellers, allowable rotor travel within the bearing should be minimized. Considering these facts in mind, a feasible configuration of foil bearing cartridge for micro turbomachinery is proposed in Fig. 8, where bearing 2 provides loading to bearings 1 and 3, and vice versa. Hatched structure corresponds to the bearing sleeve in Fig. 4. Major advantage of LIGA process over precision machining is a controllability of geometry of inner bump foil layers to off-centered from the bearing sleeve at sub-micron level and high repeatability. This advantage applies also to tilting pad gas bearings; much higher stability was observed beyond 1Mrpm if the tilting pad bearing is loaded beyond the rotor weight.

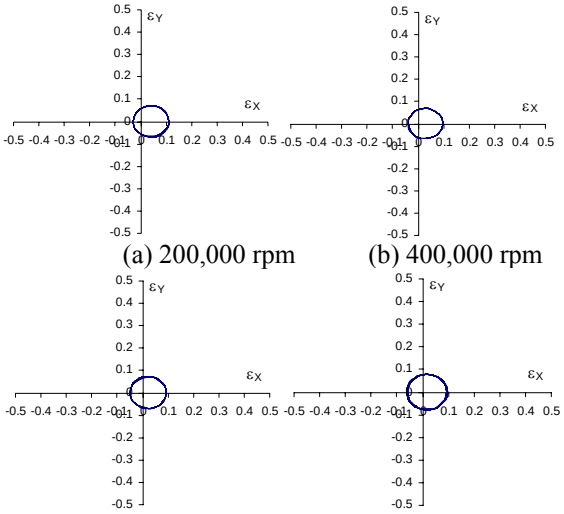

(a) 200,000 rpm (b) 400,000 rpm

(c) 600,000 rpm (d) 800,000 rpm

Figure 5 – Selected orbits for tilting pad gas bearings

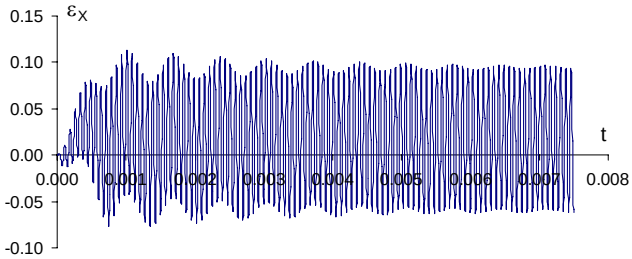

Figure 6 –Simulated time trace of ε_X for tilting pad gas bearing at 800,000 rpm

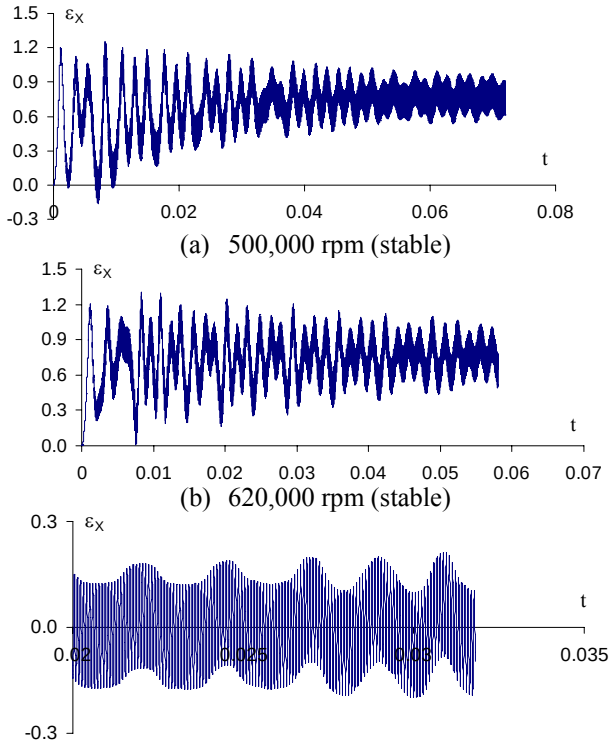

(a) 500,000 rpm (stable)

(b) 620,000 rpm (stable)

(c) 660,000 rpm (unstable)

Figure 7- Selected time traces of ε_X for foil bearing with external load of 0.5N

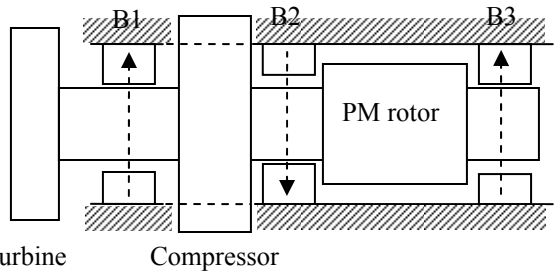

Figure 8 – Arrangement of loaded foil bearings, arrows indicate the direction of loadings

ACKNOWLEDGMENTS

This project is partially funded from US National Science Foundation through REU for Development of Microturbomachinery and Texas Engineering Experiment Station.

REFERENCES

[1] Epstein A. H., 2004, "Millimeter-Scale, Micro-Electro-Mechanical Systems Gas Turbine Engines," ASME Journal of Engineering for Gas Turbines and Power, **126**(2), pp. 205-226.

[2] Isomura, K., Tanaka, S., Togo, S., Esashi, M., 2005, "Development of high-speed micro-gas bearings for three-dimensional micro-turbo machines," J. Micromech. Microeng. **15**, pp. 222-227.

[3] Yongbok Lee, Keun Ryu, Chang-Ho Kim, 2004, "Preliminary Test Results of Rotordynamic Characteristics for 100 Watts class Micro Power System," Proceedings of Power MEMS 2004

[4] www.miti.cc/foil-bearings.html

[5] Sim, K., Kim, D., 2006, "Design of Flexure Pivot Tilting Pads Gas Bearings for High-speed Oil-Free Micro Turbomachinery," ASME Journal of Tribology, in print.

[6] Sim, K., Kim, D., 2006, 2006, "Stability Analyses on Flexure Pivot Tilting Pad Gas Bearings for Microturbomachinery," ASME Paper IJTC 2006-12158

[7] Kim, D., Lee, S., Bryant, M. D., Ling, F. F., 2004, "Hydrodynamic Performances of Gas Microbearing", ASME Journal of Tribology, **126**(4), pp.711-718Daejong Kim,

[8] http://www.grc.nasa.gov/WWW/Oilfree/bearings.htm

[9] Ehrfeld, W., Hessel, V., Lowe, H., Schilz, C., Weber, L., 1999, "Materials of LIGA Technology," Springer Microsystem Technologies, **5**, pp. 105–112

[10] Hemker, K. J. and Last, H., 2001, "Microsample Tensile Testing of LIGA Nickel for MEMS Applications", Materials Science and Engineering A, **319-321**, pp. 882-886

[11] Goods, S. H., Kelly, J.J., Yang, N., 2004, "Electrodeposited Nickel–Mnganese: An Alloy for Microsystem Applications," Springer Microsystem Technologies, **10**, pp.498–505

[12] Susumu Arai,a, Morinobu Endo, Tomoyuki Sato, Atsushi Koide, 2006, "Fabrication of Nickel–Multiwalled Carbon Nanotube Composite Films with Excellent Thermal Conductivity by an Electrodeposition Technique," Electrochemical and Solid-State Letters, **9** (8), pp. C131-C133

[13] Timoshenko, S. P., and Goodier, J. N., 1970, *Theory of Elasticity*, McGraw-Hill Co., New York, pp. 80-83.

[14] Kim, D., 2006, "Parametric Studies on Static and Dynamic Performance of Air Foil Bearings with Different Top Foil Geometries and Bump Stiffness Distributions," Accepted to ASME Journal of Tribology.

[15] Salehi, M., Heshmat, H., and Walton, J. F., 2003,"On the Frictional Damping Characteristics of Compliant Bump Foils," ASME Journal of Tribology, **125**, pp. 804-813.

[16] Rubio, D. and San Andrés , L., 2005, Structural Stiffness, Dry-friction Coefficient and Equivalent Viscous Damping in a Bump-Type Foil Gas Bearing," ASME Paper GT2005-68384.

[17] Song, J. and Kim, D, 2006, "Foil Bearing with Compression Springs: Analyses and Experiments," ASME Paper IJTC2006-12160.

[18] Chapra, S. C. and Canale, R. P., 1989, *Numeical methods for Engineers*, McGraw-Hill, New York, pp. 631-634.